Magnetic catalysis and diamagnetism from pion fluctuations

Jie Mei,[1,2,3,*] Rui Wen,[1] Shijun Mao,[4] Mei Huang,[1] and Kun Xu[1,†]

[1]*School of Nuclear Science and Technology, University of Chinese Academy of Sciences, Beijing, 100049, People's Republic of China*

[2]*School of Physical Sciences, University of Chinese Academy of Sciences, Beijing 100049, People's Republic of China*

[3]*Institute of High Energy Physics, Chinese Academy of Sciences, Beijing, 100049, People's Republic of China*

[4]*School of Physics, Xi'an Jiaotong University, Xi'an, Shaanxi 710049, People's Republic of China*

(Received 8 March 2024; accepted 26 July 2024; published 19 August 2024)

In the framework of the Nambu–Jona-Lasinio model beyond mean field approximation, the effects of pion fluctuations on (inverse) magnetic catalysis and magnetic susceptibility are studied. The negative magnetic susceptibility at low temperature is observed when contributions from both neutral and charged pions are taken into account. In the weak field approximation, it is observed that at finite temperature, the magnetic inhibition effect in the chiral limit, resulting from the difference between the transverse and longitudinal velocities of neutral pions, converts to weak magnetic catalysis when considering a nonzero current quark mass. Moreover, the magnetic catalysis is amplified by the charged pions. Therefore, no inverse magnetic catalysis is observed when considering pion fluctuations.

DOI: 10.1103/PhysRevD.110.034024

I. INTRODUCTION

The investigation of the response of quark matter to a uniform magnetic field background has been a hot topic for the last decade, see reviews [1–5]. In the experimental aspect, a strong but transient magnetic field can be generated in the initial stage of heavy ion collisions (HIC), which was believed to be the strongest magnetic field ever created, with the strength of $eB \sim 10^{18-20}$ Gauß and life time of 10^{-22} sec [6–10]. In the theoretical aspect, the interplay between a magnetic field and quantum chromodynamics (QCD) can lead to various novel behaviors and can be used as a probe to investigate the inner structure of quark matter.

The surge of the interest in studying the influence of magnetic field to a equilibrium system starts from two abnormal results from a lattice QCD group's *ab initio* calculation, (i) although the vacuum quark mass is enhanced by the magnetic field, the chiral critical temperature decrease with the increasing of it, which is called inverse magnetic catalysis (IMC), (ii) the magnetic susceptibility is negative at low temperature while positive at high temperature [11–16]. These results disagree with most of the effective model predictions at that time, for instance, the standard Nambu-Jona-Lasinio (NJL) model and linear-σ model with quark (quark-meson model) under mean-field approximation [17,18].

Numerous studies have been conducted to elucidate the IMC and diamagnetic effects. These investigations have explored various mechanisms, including magnetic inhibition resulting from fluctuations of neutral pions [19], chirality imbalance stemming from sphaleron transitions or instanton-anti-instanton pairings [20,21], and the influence of the running coupling constant in the presence of a magnetic field [22]. Some groups tried to include the anomalous magnetic moment effect [23–30] or the effect of tensor channel [26] in the NJL model to reproduce the IMC or diamagnetism. By considering the running coupling with eB-dependence fitted by lattice QCD data, the IMC result can be successfully reproduced in [31–38]. Hadron resonance gas (HRG) model, where the hadrons are assumed as point-like particles with no interaction in between, can also reproduce diamagnetic result at low temperature region [39,40]. Functional continuum field approaches, such as the functional renormalization group (FRG), Dyson-Schwinger equations (DSE), and holographic QCD models also have made great efforts on both the effective models [39,41–48] and QCD theory [49–51]. In general, the understanding of the IMC and diamagnetic effects remains an open question.

*Contact author: meijie22@mails.ucas.ac.cn

†Contact author: xukun21@ucas.ac.cn

Most of the work in the NJL model was done based on the mean-field approximation which only considers the lowest-order in $1/N_c$ expansion [52]. In next-to-leading order of this expansion, the feedback effect from mesons is taken into consideration [53,54]. Generally, mean field approximation for quark together with random phase approximation for meson works well to describe the thermodynamic properties of QCD matter in absence of magnetic field. For the puzzle of IMC and diamagnetism, the feedback from mesons can be part of the solution, given that they are influenced by magnetic field in both direct (for charged mesons) and indirect (for neutral mesons) manners [38,55–61]. In Refs. [19,62,63], the feedback effect from π_0 with a physical propagating velocity is included in the chiral limit, giving an IMC result. Besides, in the (Polyakov-loop extended) quark-meson model, the meson fluctuations, especially the light pion contributions, lead to the diamagnetism [39,42]. In our calculation, we investigated beyond mean field by including the effect from both π_0 and $\pi^{\pm}$ with and without finite propagating velocities, and consider a physical situation where chiral symmetry is explicitly broken, to see their role in (inverse) magnetic catalysis and magnetic susceptibility.

This paper is arranged as follows: In Sec. II we introduce the calculating procedure in beyond mean-field NJL model in the manner of weak-field expansion. In Sec. III, we give the numerical results for eB-dependence of critical temperature T_c and magnetic susceptibility followed by a summary and discussion in Sec. IV.

II. THE NJL MODEL

We start with the Lagrangian of SU(2) NJL model in the presence of a uniform magnetic field,

$$\mathcal{L} = \bar{\psi}(i\gamma^\mu D_\mu - \hat{m})\psi + G[(\bar{\psi}\psi)^2 + (\bar{\psi}i\gamma_5\vec{\tau}\psi)^2]. \quad (1)$$

Here, ψ is two-flavor quark field $\psi = (u, d)^T$, $\hat{m}$ is the quark current mass matrix $\hat{m} = \mathrm{diag}(m_u, m_d)$ with $m_u = m_d = m_0$, which explicitly breaks the chiral symmetry, and τ_i is ith component of Pauli matrices. The covariant derivative $D_\mu = \partial_\mu - iQA_\mu$ coupling quarks with electric charge $Q = \mathrm{diag}(q_u, q_d) = \mathrm{diag}(2/3e, -1/3e)$ to a gauge field $\mathbf{B} = \nabla \times \mathbf{A}$. In this article, we choose the Landau gauge, where the potential $A_\mu = (0, 0, Bx_1, 0)$.

In Schwinger scheme, the translational invariance for a charged particle is broken by the magnetic field, dividing the quark propagator into two parts, namely, the Schwinger phase part and the Fourior transformation of translational invariant part.

$$S_f(x, y) = e^{i\Phi_f(x_\perp, y_\perp)} \int \frac{d^4k}{(2\pi)^4} e^{-ik(x-y)} \tilde{S}_f(k_\perp, k_\parallel). \quad (2)$$

Here, the parallel and perpendicular components of the four-dimensional coordinate and momentum are written as $x_\perp = (x_1, x_2)$, $k_\perp = (k_1, k_2)$ and $k_\parallel = (k_0, k_3)$. The quark Schwinger phase in Landau gauge reads

$$\Phi_f(x_\perp, y_\perp) = \frac{q_f B}{2}(x_1 + y_1)(x_2 - y_2), \quad (3)$$

which is gauge-dependent. The detailed forms of Schwinger phase in different gauges can be found in [4,64]. To include the effect of Schwinger phase in weak field expansion, one can shift the zeroth order of it. In Sec. III, we will explain that the missing of Schwinger phase does not affect the qualitative conclusion of this work, and we neglect Schwinger phase in the following.

In the weak magnetic field limit, the quark propagator in momentum space can be expanded in the power of $(q_f B)$, and reads

$$\begin{aligned} &i\tilde{S}_f(k_\perp, k_\parallel) \\ &= i\frac{m_q + \not{k}}{k^2 - m_q^2} - (q_f B)\frac{\gamma_1\gamma_2(m_q + \not{k}_\parallel)}{(k^2 - m_q^2)^2} \\ &\quad - 2i(q_f B)^2 \frac{k_\perp^2(m_q + \not{k}_\parallel) + \not{k}_\perp(m_q^2 - k_\parallel^2)}{(k^2 - m_q^2)^4} + \mathcal{O}(q_f B)^3 \\ &= i\tilde{S}^{(0)} + (q_f B)i\tilde{S}^{(1)} + (q_f B)^2 i\tilde{S}^{(2)} + \mathcal{O}(q_f B)^3 \end{aligned} \quad (4)$$

where the contributions of transverse and parallel momentum are considered separately. Here, m_q is the constituent quark mass, which is the same value for both u and d flavor. We use the notation,

$$\begin{aligned} (a \cdot b)_\parallel &= a^0 b^0 - a^3 b^3, \\ (a \cdot b)_\perp &= a^1 b^1 + a^2 b^2, \end{aligned} \quad (5)$$

hence $k^2 = k_\parallel^2 - k_\perp^2$.

A. Mean field approximation

In mean field approximation, the thermodynamic potential of the system at finite temperature and under external magnetic field B takes the form of:

$$\Omega_{\mathrm{MF}}(T, B) = \frac{(m_q - m_0)^2}{4G} + \Omega_q(T, B), \quad (6)$$

with the contribution from quarks:

$$\Omega_q(T, B) = \mathrm{Tr}_{\{c,f,s,x\}} \ln\left(\frac{1}{T} S^{-1}(x, x)\right). \quad (7)$$

The trace operation is carried out over color (c), flavor (f), spinor (s) degrees of freedom, as well as over the four-dimensional coordinate (x). $S^{-1}(x, x)$ is the inverse of quark propagator in coordinate space.

To determine the effective quark mass, we have to find the ground state by locating the global minimum of the thermodynamic potential

$$\frac{\partial \Omega_{\rm MF}(T,B)}{\partial m_q} = 0,$$
$$\frac{\partial^2 \Omega_{\rm MF}(T,B)}{\partial m_q^2} \geq 0, \tag{8}$$

which leads to the gap equation

$$m_0 = m_q - 2G\mathrm{Tr}_{\{c,f,s,k\}}[i\tilde{S}(k)]. \tag{9}$$

Inserting Eq. (2) into Eq. (9) and apply the summation over Matsubara frequency, we can obtain the weak-field expansion version of gap equation

$$m_q\left(1 - 2GN_c\sum_f\left(I_1^{(0)} + (q_fB)^2 I_1^{(2)} + \mathcal{O}(q_fB)^4\right)\right) = m_0, \tag{10}$$

with

$$I_1^{(0)} = -4\int \frac{d^3k}{(2\pi)^3}\mathcal{F}_{(1)}(m_q^2), \tag{11}$$

$$I_1^{(2)} = 8\int \frac{d^3k}{(2\pi)^3}k_\perp^2\mathcal{F}_{(4)}(m_q^2). \tag{12}$$

There is no contribution from odd terms of $I_1^{(n)}$ after performing the trace in spinor space, which agrees with symmetry analysis. The contributions from higher orders of magnetic field are neglected. Here we define the fermionic threshold functions

$$\mathcal{F}_{(n)}(m_q^2) \equiv T\sum_{n_T}\frac{1}{(k^2 - m_q^2)^n}, \tag{13}$$

then it is straightforward to obtain

$$\mathcal{F}_{(1)} = \frac{1}{2E_q}\left(1 - 2n_f(m_q^2)\right), \tag{14}$$

$$\mathcal{F}_{(n+1)} = \frac{1}{n}\frac{\partial}{\partial m_q^2}\mathcal{F}_{(n)}. \tag{15}$$

Here, $n_f(m_q^2)$ is fermionic distribution functions and quark energy dispersion relation $E_q = \sqrt{\mathbf{k}^2 + m_q^2} = \sqrt{k_3^2 + k_\perp^2 + m_q^2}$.

Correspondingly, the quark part of thermodynamic potential can also be rewritten in this weak-field expansion manner

$$\Omega_q = \Omega_q^{(0)} + \sum_f (q_fB)^2\Omega_q^{(2)} + \mathcal{O}(q_fB)^4, \tag{16}$$

$$\Omega_q^{(0)} = -2N_cN_f\int\frac{d^3k}{(2\pi)^3}[E_q + 2T\ln(1 + e^{\frac{-E_q}{T}})], \tag{17}$$

$$\Omega_q^{(2)} = -\frac{4N_c}{3}\int\frac{d^3k}{(2\pi)^3}k_\perp^2\mathcal{F}_{(3)}(m_q^2). \tag{18}$$

B. Meson section

In the NJL model, mesons are treated as quantum fluctuations above the mean field. Through the random phase approximation (RPA) method, the meson propagator can be expressed in terms of the irreducible polarization function or quark bubble,

$$\Pi_M(q^2) = i\int\frac{d^4k}{(2\pi)^4}\mathrm{Tr}_{\{c,f,s\}}[\Gamma_M^*\tilde{S}(k)\Gamma_M\tilde{S}(k-q)], \tag{19}$$

with the meson vertex

$$\Gamma_M = \begin{cases} 1, & M = \sigma \\ i\gamma_5\tau_+, & M = \pi_+ \\ i\gamma_5\tau_-, & M = \pi_- \\ i\gamma_5\tau_3, & M = \pi_0, \end{cases}, \tag{20}$$

where $\tau_\pm$ is determined by $\tau_\pm = (\tau_1 \pm i\tau_2)/\sqrt{2}$. By inserting Eq. (2) into Eq. (19), we can get the polarization function for π_0 in the weak field approximation

$$\Pi_{\pi_0}(q^2) = N_c\sum_f[\Pi^{00} + (q_fB)^2(2\Pi^{20} + \Pi^{11})], \tag{21}$$

with definition

$$\Pi^{lm}(q^2) = i\int\frac{d^4k}{(2\pi)^4}\mathrm{Tr}_{\{s\}}[i\gamma_5\tilde{S}^{(l)}(k)i\gamma_5\tilde{S}^{(m)}(k-q)]. \tag{22}$$

After performing the trace in spinor space, the contribution of Π^{10} and Π^{01} vanishes. The calculation for Eq. (22) is straightforward but tedious. For the polarization function for charged pions, it has the similar form as the neutral pion case,

$$\Pi_{\pi_\pm}(q^2) = 2N_c\left[\Pi^{00} + (q_uB)(q_dB)\Pi^{11} + \sum_f(q_fB)^2\Pi^{20}\right]. \tag{23}$$

Again, the contribution of Π^{01} vanishes after carrying out the trace in spinor space.

Via taking the bubble summation in random phase approximation, the effective propagator for a meson M can be constructed by

$$U_M = \frac{2G}{1 - 2G\Pi_M}, \tag{24}$$

and the pole mass $m_{\rm pole}$ (static solution, setting $q_1 = q_2 = q_3 = 0$) and the screening masses $m_{{\rm scr},i}$ in q^i direction (setting $q_0 = 0$, and $q_j = 0$ for $j \neq i$) can be solved by following equations, correspondingly,

$$1 - 2G\Pi_M(q_0^2 = m_{\rm pole}^2, 0) = 0 \tag{25}$$

and

$$1 - 2G\Pi_M(0, q_i^2 = -m_{{\rm scr},i}^2) = 0. \tag{26}$$

The detailed calculation for the polarization function in weak-field expansion are listed in Appendix A. It should be noted that when meson pole (screening) mass exceeds the threshold of the mass sum of its constituent quarks, the meson undergoes a Mott transition and a finite width ($m_M \to m_M - i\frac{\Gamma}{2}$) should be taken into consideration. The meson mass and its width can be determined by the corresponding complex equations. In this paper, we work in the temperature region where pions are still bound state particles.

C. Beyond mean-field approximation

We go beyond the mean-field approximation by using the $1/N_c$ expansion [53,54]. Another self-consistent beyond mean-field method in the NJL model is the FRG approach [65,66]. By including the next-to-leading order of $1/N_c$ expansion, meson degrees of freedom are self-consistently introduced. The thermodynamic potential of the quark-meson plasma [54] can be rewritten as

$$\Omega = \frac{(m_q - m_0)^2}{4G} + \Omega_q + \sum_M \Omega_M. \tag{27}$$

In pole approximation, the meson contribution in thermodynamic potential with vanishing magnetic field takes the form,

$$\Omega_\pi = \int \frac{d^3k}{(2\pi)^3}\left[\frac{E_\pi}{2} + T\ln\left(1 - e^{-E_\pi/T}\right)\right], \tag{28}$$

with meson energy dispersion relation

$$E_\pi = \sqrt{m_{\pi,\rm pole}^2 + (\mathbf{v}\cdot\mathbf{k})^2}. \tag{29}$$

As shown in [67–71], $\mathbf{v}$ in Eq. (29) represents the propagating velocity for the corresponding meson, whose ith component has the form of [68–71]

$$v_i = \frac{m_{M,\rm pole}}{m_{M,{\rm scr},i}}. \tag{30}$$

For neutral pion, when we consider its behaviors in the hadron level, it has no interaction with magnetic field at all. However, in a model in quark level like NJL model, its magnetic field-sensitive constituent quark will contribute to the variation of π_0 mass and the splitting of its propagating velocity in parallel and perpendicular directions, leading to the new form of energy dispersion relation

$$E_{\pi_0} = \sqrt{m_{{\rm pole},\pi_0}^2 + v_\perp^2 k_\perp^2 + v_\parallel^2 k_3^2}, \tag{31}$$

which is believed to be responsible for the IMC effect in the chiral limit, as in [19,62,63]. In absence of a uniform magnetic field, the neutral pion π_0 and charged pions $\pi_\pm$ are isospin triplet that share the same form of thermodynamic potential. When a magnetic field is turned on, the charged pions obtain extra masses from magnetic field, and decouple from neutral pion, which means we should consider their effect separately. For charged pions, the magnetic field not only alter their pole masses and propagating velocities, but also change the momentum in perpendicular directions from thermodynamic potential and energy dispersion relation into discrete Landau levels,

$$\Omega_{\pi_\pm} = \sum_{n=0}^{\infty}\frac{|eB|}{2\pi}\int_{-\infty}^{\infty}\frac{dk_3}{2\pi}\left[\frac{E_{\pi_\pm}}{2} + T\ln\left(1 - e^{-E_{\pi_\pm}/T}\right)\right], \tag{32}$$

$$E_{\pi_\pm} = \sqrt{m_{\pi_\pm}^2 + v_\perp^2(2n+1)|eB| + v_\parallel^2 k_3^2}. \tag{33}$$

Here we use the strong-field form of charged pion's energy dispersion relation, to take the cyclotron motion into consideration. $m_{\pi_\pm}$ refers to the mass obtained by solving the pole equation with zero external momentum, and both $v_\parallel$ and $v_\perp$ are extracted from results in weak field limit. It should be mentioned that in strong field formulation, the velocity in transverse direction is ill-defined, since the momentum in corresponding direction has become separate Landau levels. To guarantee that in weak field limit Eq. (33) can reduced back to Eq. (29), we keep this coefficient in this work. In the following, the "propagating velocity" of $\pi_\pm$ at finite magnetic field should be understood as a ratio before Landau level. In Appendix B, we try to understand the definition of v better through an demonstrative analysis on meson's two-point correlation function.

Now with the complete form of thermodynamic potential beyond mean field, we can get the new constituent quark mass from the corresponding gap equation with the feedback effect from meson,

$$m_q\left(\frac{1}{4G}+\frac{\partial\Omega_q}{\partial m_q^2}+\sum_M\frac{\partial\Omega_M}{\partial m_q^2}\right)=\frac{m_0}{4G}. \tag{34}$$

Comparing the mean field quark mass m_{MF} from Eq. (9) with the newly obtained quark mass m_q from Eq. (34), there is a mass difference which comes from the quantum fluctuations above the mean field. Following the procedure described in [54], the meson contribution in thermodynamic potential can be expanded in power of $(m_q^2-m_{\mathrm{MF}}^2)$,

$$\Omega_M=\sum_{n=0}^{\infty}\frac{1}{n!}\frac{\partial^n\Omega_M}{(\partial m_q^2)^n}\bigg|_{m_q^2=m_{\mathrm{MF}}^2}(m_q^2-m_{\mathrm{MF}}^2)^n. \tag{35}$$

To simplify the calculation, we only consider the first two terms of the above series, where the leading order term vanishes and only the next-to-leading order term has nonzero contribution, then we get the practical form of gap equation,

$$m_q\left(\frac{1}{4G}+\frac{\partial\Omega_q}{\partial m_q^2}+\sum_M\frac{\partial\Omega_M}{\partial m_q^2}\bigg|_{m_q^2=m_{\mathrm{MF}}^2}\right)=\frac{m_0}{4G}. \tag{36}$$

In the previous beyond-mean-field calculation with nonvanishing magnetic field, most works focus on the effect of neutral pions in the chiral limit, giving a conclusion that including a neutral pion with a physical propagating velocity may cause inverse magnetic catalysis effect. Those calculations stand because they are working in strong field limit, where charged pion gained a large mass from magnetic field and hence their contribution in the distribution function can be neglected. In this work, however, we work in weak field limit with $eB\sim m_\pi^2$. The mass disparity between neutral and charged pions is not significant enough, and the contributions from charged pions should not be overlooked. In the next section, we will investigate how the neutral pion and charged pions affect the chiral condensate and magnetic susceptibility.

III. NUMERICAL RESULTS

In order to analyze the roles of neutral and charged pions in (inverse) magnetic catalysis and magnetic susceptibility, we consider the following four cases: case 0: Mean field approximation; case I: only neutral pion contribution; case II: only charged pions contribution; case III: both neutral and charged pions contribution, which are listed in Table I. We will also investigate the effect with and without finite pion propagating velocities separately.

Because of the contact interaction in the NJL model, the ultraviolet divergence cannot be eliminated through renormalization, and a proper regularization scheme is needed. In our work, we apply the gauge invariant Pauli-Villars regularization [62], which can guarantee the law of causality and effectively avoid the unphysical oscillation at finite magnetic field. Other schemes, like proper-time regularization scheme and magnetic field independent regularization (MFIR) [59,60], which separates the vacuum and magnetic contribution, are also effective when dealing with system under a uniform magnetic field. By fitting the physical quantities, chiral condensate $\langle\bar\psi\psi\rangle=(-250\ \mathrm{MeV})^3$, pion decay constant $f_\pi=93$ MeV in vacuum, we fix the current mass of light quarks $m_0=5$ MeV, and obtain the parameter $\Lambda=1127$ MeV. For different cases, the coupling constants are given in Table I.

TABLE I. Coupling constants in different cases in and beyond mean field approximation.

Case	Included mesons	$G\Lambda^2$
0	None	4.37
I	π_0 only	4.81
II	$\pi_\pm$ only	5.36
III	$\pi_0,\pi_\pm$	6.05

The full calculating procedure is as follows: (1) we first calculate the mean field gap equation Eq. (9) to get the mean field quark mass m_{MF} before substituting it into the pole equation Eq. (25), where we can get the pole and screening masses of π_0 and $\pi_\pm$, and hence the corresponding propagating velocity in longitudinal and transverse directions. (2) Inserting the pion dispersion relation obtained above into the beyond-mean-field thermodynamic potential Eq. (27) and gap equation Eq. (34), we can finally get the numerical result of order parameter m_q and magnetic susceptibility. In this work, we employ this systematic step-by-step approach to go beyond the mean field approximation, and more self-consistent ways to go beyond mean field in absence of magnetic field are given in [72,73].

In the case of explicit chiral symmetry breaking, the pseudo Nambu-Goldstone modes π have a finite mass, making them propagating with a velocity lower than the speed of light at finite magnetic field and finite temperature. Due to the qualitative similarity in the behaviors of pion masses and propagating velocities across different cases, in Figs. 1–3 we will choose the case that exhibits the most conclusive results to highlight the distinctions arising from a relatively weak magnetic field.

A. Meson properties

Here we start by examining the characteristics of neutral and charged pion masses at finite temperature and magnetic field. Figure 1 demonstrates the magnetic field dependence of π_0 and $\pi_\pm$ masses at zero temperature. We use the weak field expansion and only calculate to $eB=3m_\pi^2$ with $m_\pi^2=0.0179\ \mathrm{GeV}^2$. For π_0 mass, it decreases with the increase of the magnetic field, while for the ground state

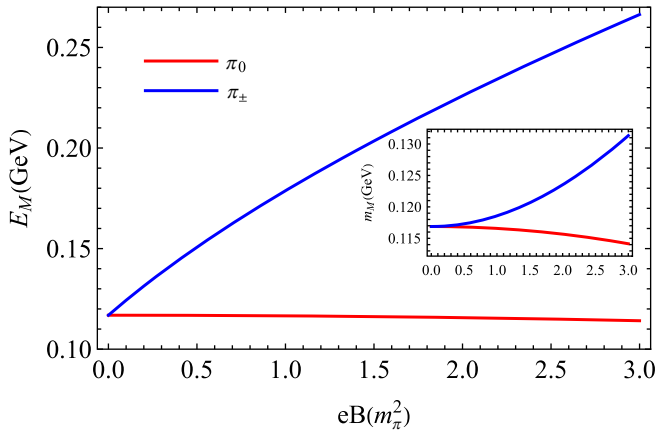

FIG. 1. Neutral (red solid line) and charged (blue solid line) pion masses beyond mean field approximation in case III as a function of magnetic field, with vanishing temperature.

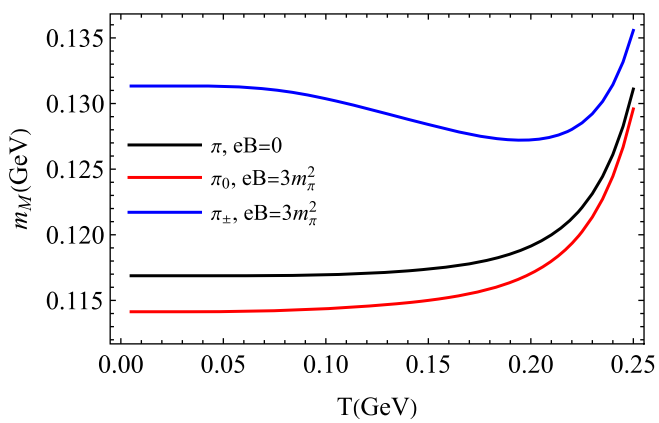

FIG. 2. Pion mass beyond mean field approximation in case III as a function of temperature with vanishing magnetic field.

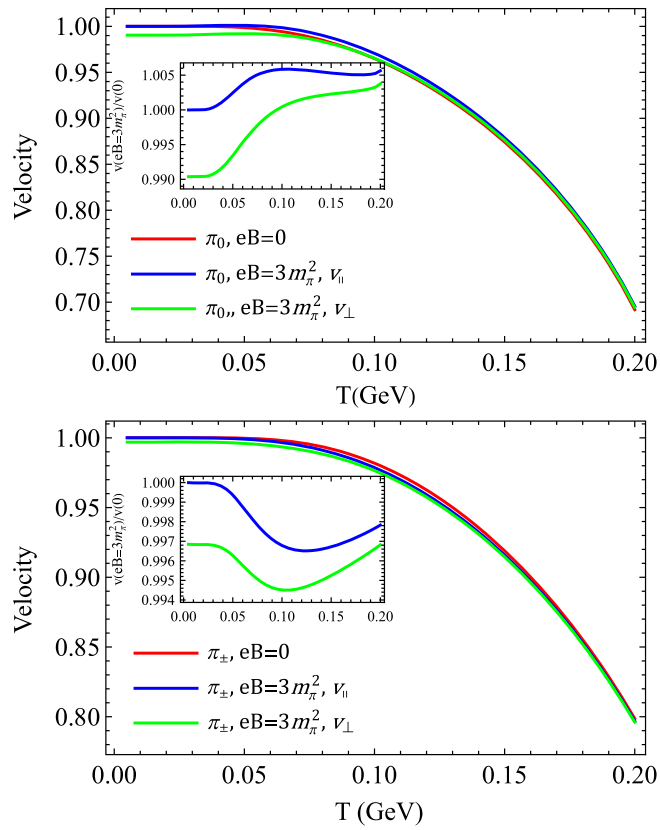

FIG. 3. Propagating velocity (ratio) of π_0 (upper panel) and $\pi_\pm$ (lower panel) beyond mean field in case I and case II as a function of temperature at different magnetic field in the chiral symmetry breaking phase. The inlaid subfigure shows the ratio of velocities at $eB = 3m_\pi^2$ and $eB = 0$ in corresponding directions.

energy of $\pi_\pm$, which is given by $E_{\pi_\pm} = \sqrt{m_{\pi_\pm}(eB)^2 + eB}$, it increases with the magnetic field, showing an opposite tendency. If we consider π_0 as a charge-neutral point-like particle, it should remain unaffected by external magnetic field, while in the NJL model where mesons are considered as composite particles made of quark anti-quark, π_0 mass changes with the changing of quark condensate. From the Nambu-Goldstone theorem, since the explicit breaking of chiral symmetry will get more "explicit" with the restoration of chiral symmetry, the mass of the pseudo-Goldstone boson π_0 should generally decreases with magnetic field, which is consist with our numerical result. A uniform magnetic field breaks the isospin symmetry between u and d quarks, and $\pi_\pm$ gained mass from magnetic field, which is qualitatively consist with the pointlike approximation (PLA) result, i.e., $E_{\pi_\pm}^{\mathrm{PLA}}(B) = \sqrt{m_{\pi_\pm}^2(B=0) + eB}$.

In Fig. 2 we show the temperature-dependence of $m_{\pi_0,\mathrm{pole}}$ and $m_{\pi_\pm}$ at $eB = 0$ and $eB = 3m_\pi^2$. At vanishing magnetic field, neutral and charged pions share the same mass. As the temperature gets higher, pion mass increases with the restoration of chiral symmetry, which is in agreement with the analysis of Nambu-Goldstone theorem. At $eB = 3m_\pi^2$, the pole masses of neutral and charged pions split. It should be noticed that at high temperature region, the system is thermalized and the splitting between $m_{\pi_0,\mathrm{pole}}$ and $m_{\pi_\pm}$ becomes smaller.

Figure 3 shows longitudinal and transverse velocities of both π_0 and $\pi_\pm$ as a function of the temperature at $eB = 0$ and $eB = 3m_\pi^2$. At vanishing magnetic field, both π_0 and $\pi_\pm$ exhibit isotropic behavior and their velocities decrease with the increase of temperature, since the temperature leads to a breakdown of Lorentz symmetry in boost transformations. When a magnetic field is turned on, we can clearly observe the splitting between the longitudinal and transverse velocities for both π_0 and $\pi_\pm$. For transverse velocity, it gets lower than the vanishing magnetic field scenario, while for longitudinal velocity, it is generally the same as that in the vanishing magnetic field case at low temperature region. When the temperature gets higher, the splitting between the longitudinal and transverse velocities induced by magnetic field gets melted and the system tends

to become isotropic again. This thermalization phenomenon is also observed in the strong field case, e.g., [71]. When the temperature increases, the velocity of neutral pion at $eB = 3m_\pi^2$ gets larger than that at $eB = 0$, since the neutral pion becomes lighter at higher magnetic field. The behavior of $\pi_\pm$ is basically the same as the neutral pion case, except that with the increase of magnetic field strength, the propagating velocity of $\pi_\pm$ tends to be smaller, given that the charged pion mass is increased by the magnetic field.

It should be noted that in the chiral limit, the behavior of propagating velocities appears to exhibit the opposite trend, where the longitudinal velocity is always exactly the same as the speed of light, the transverse velocity gets lower as temperature increases. This discrepancy between transverse and longitudinal velocities was believed to lead to magnetic inhibition, which gives the IMC result in the chiral limit [19,62,63].

B. Chiral condensate beyond mean field

Now with the pole mass, screening masses and propagating velocities of π_0 and $\pi_\pm$ obtained in the mean-field approximation, we can insert them into the beyond-mean field thermodynamic potential and gap equation to get the quark mass in cases I, II, and III. Before that, we can first calculate the effective coupling $\tilde{G}$ with

$$\frac{1}{4\tilde{G}} \equiv \frac{1}{4G} + \sum_M \frac{\partial \Omega_M}{\partial m_q^2}\bigg|_{m_q^2 = m_{\mathrm{MF}}^2} \tag{37}$$

to investigate the feedback effect from different pion to the system. To demonstrate the influence of magnetic field on effective coupling in the whole temperature region, in Figs. 4 and 5 we show $\tilde{G}(eB = 0)$ and $\tilde{G}(eB = 3m_\pi^2)$ with the feedback from different mesons, with and without the consideration of the effect of finite pion propagating velocities.

Figure 4 shows the temperature dependence of effective coupling at different magnetic field strength with velocities $v = 1$. We start with case I in the upper panel. The effective coupling generally increases until getting close to its Mott transition point, where a plunge is observed. As shown in Eq. (37), the effective coupling is determined by the contribution from mesons. The mesonic energy dispersion relation is controlled by two different factors, i.e., the pole mass and propagating velocity. In Fig. 4, velocities are set to be the speed of light, and as demonstrated in Fig. 2, the pole mass of neutral pion is monotonically increasing with temperature, which leads to the increasing of mesonic energy and the decreasing of its contribution in the effective coupling. For the same reason, the effective coupling at higher magnetic field background always gets lower than that at vanishing magnetic field in case I. For case II and case III in the middle and lower panels, Since we are examining the impact of charged pions, the effective coupling in these scenarios actually increases with the magnetic field. This is due to the fact that charged pions exhibit an opposing and more pronounced reaction to the magnetic field. This result suggests that neglecting the finite velocity effect may weaken magnetic catalysis in case I, but strengthen it in cases II and III. Since the inclusion of the Schwinger phase does not bring qualitative change to the behavior of charged pion mass, according to [55,64], and the increment of $\pi_\pm$ masses still leads to the enhancement of effective coupling, we can conclude that the Schwinger phase will not affect our analysis.

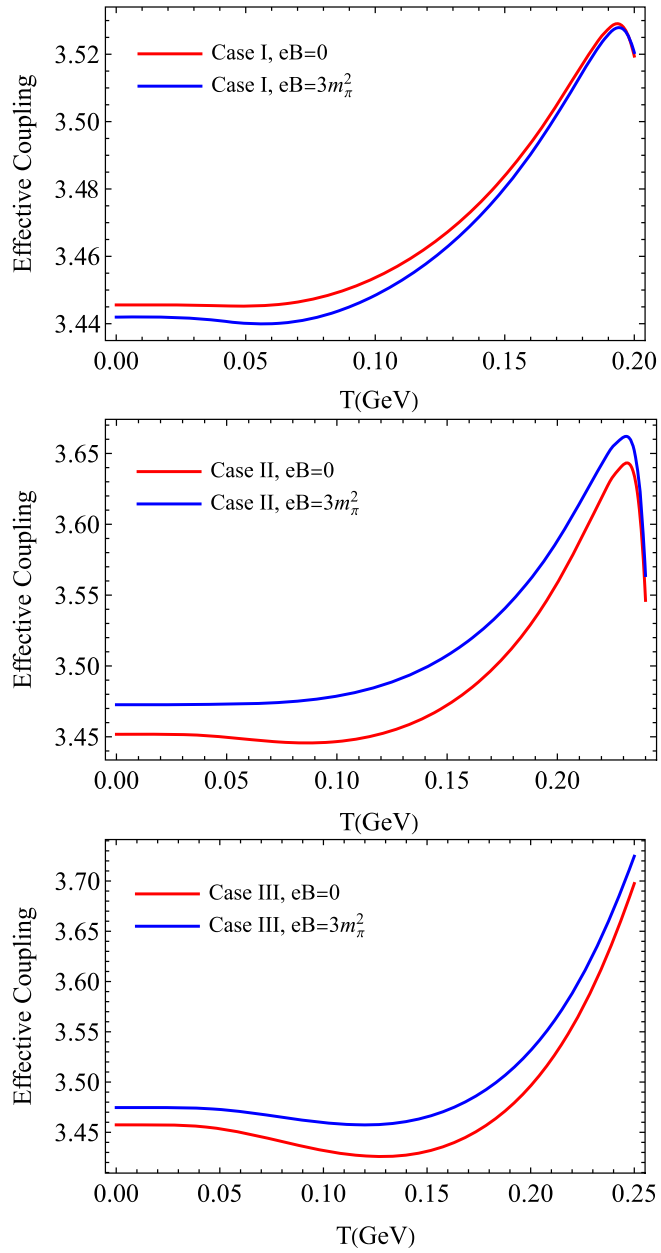

FIG. 4. Effective coupling $\tilde{G}$ at $eB = 0$ and $eB = 3m_\pi^2$ as a function of temperature in three different cases, considering constant pion propagating velocities (ratios).

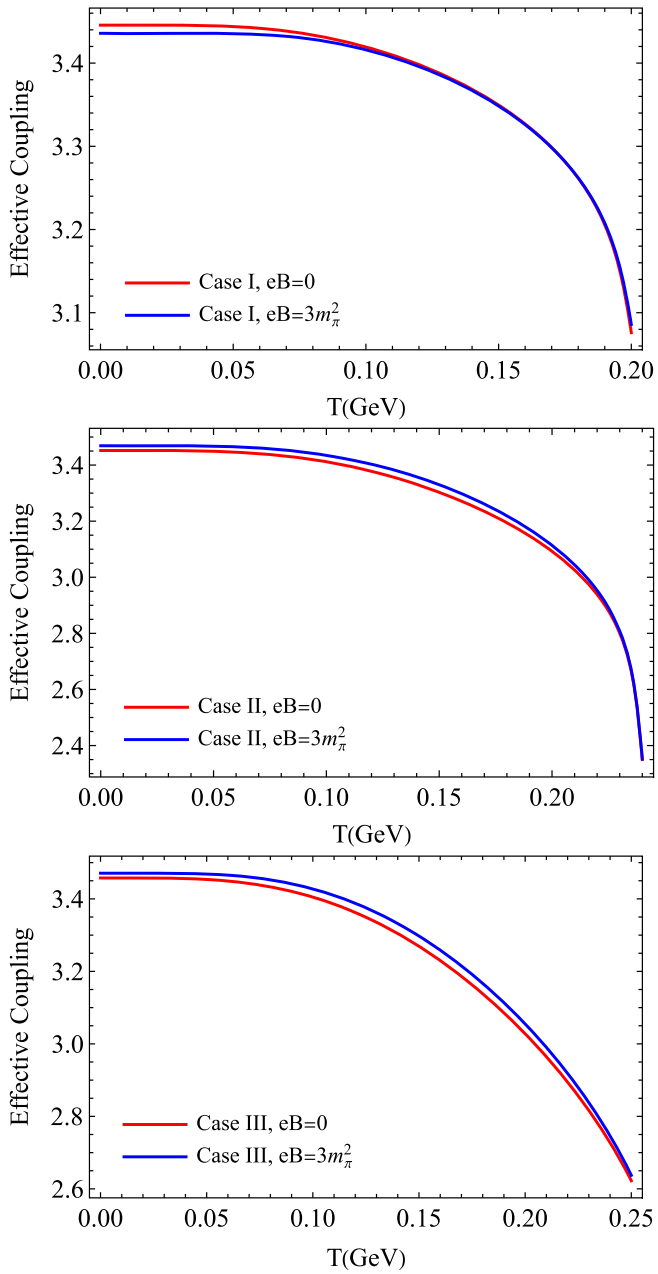

FIG. 5. Effective coupling $\tilde{G}$ at $eB = 0$ and $eB = 3m_\pi^2$ as a function of temperature in three different cases, considering pion propagating velocities (ratios) dependent on temperature and magnetic field.

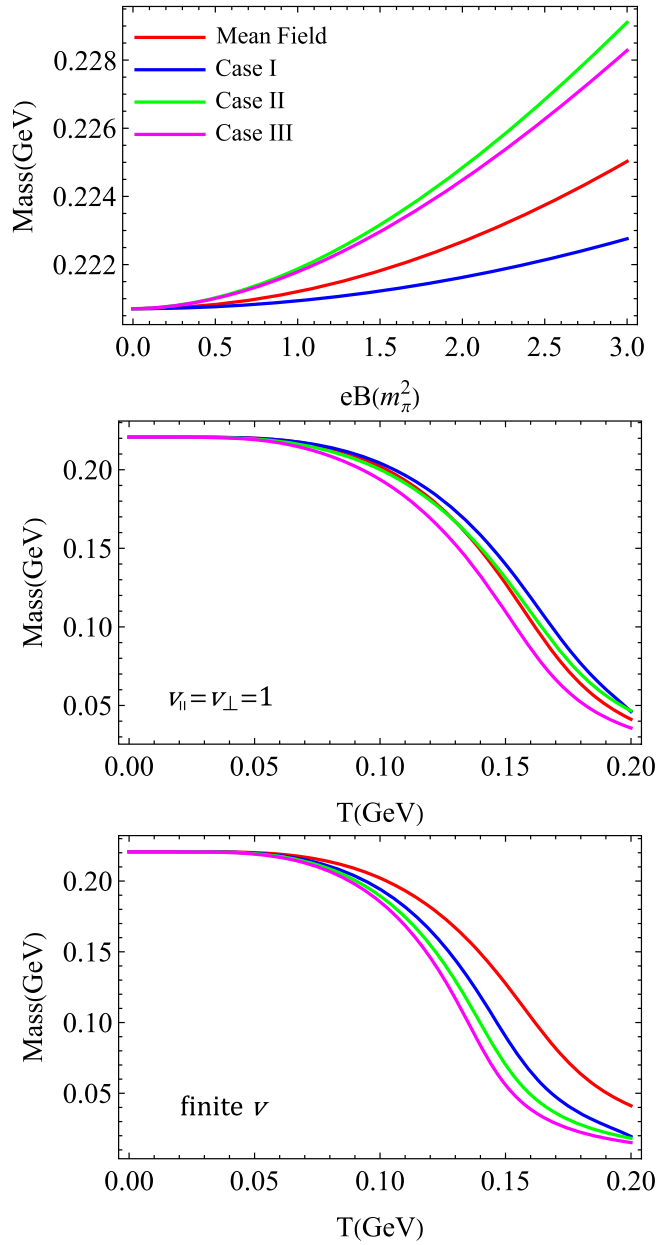

FIG. 6. Effective quark mass m_q in four different cases, as a function of magnetic field with zero temperature (upper panel) and of temperature in vanishing magnetic field with finite and constant pion propagating velocities (ratios) (middle and lower panel), with $m_\pi^2 \simeq 0.0179$ GeV^2.

Figure 5 shows the temperature dependence of effective coupling at different magnetic field strength with finite velocities. Different from the result in Fig. 4, the effective coupling in Fig. 5 monotonically decreases with the increase of temperature. This is because the drop in propagating velocities leads to a decrease in mesonic energy, which in turn increases the overall contribution from pions. We can also notice that, although the response of effective coupling to the magnetic field is qualitatively the same as in Fig. 4, the magnitude is significantly weakened. In case I, for example, the effect from magnetic field becomes indistinguishable at around temperature $T \sim 0.15$ GeV. One can also find an explanation from Figs. 2 and 3, where the changes from propagating velocities counteracts the effect of pole masses in energy dispersion relation.

In Fig. 6, we show the quark mass as a function of the magnetic field (up panel) and the temperature with pion propagating velocity $v = 1$ (middle panel) and finite v (below panel) for four cases listed in Table I. It is noticed

from the upper panel that although the constituent quark mass increases with magnetic field in all cases, the increasing rate is lower in case I with only neutral pion contribution compared to the mean-field case. The increasing rate of quark mass is significantly enhanced in both case II and case III in the case of considering the charged pion contribution. It is observed that in the middle figure where we consider the pionic velocity to be exactly the speed of light, the chiral symmetry restoration phase transition is catalyzed in case I and inverse-catalyzed in case III, while in case II the behavior of quark condensate is similar to that of mean field case. However, in the lower panel, when the propagating velocities are dependent on the temperature and magnetic field strength, in all the beyond-mean-field cases, the chiral phase transition is inverse-catalyzed, and the more pions are considered, the more inverse-catalytic the system becomes. By observing the results for different cases in Fig. 6, it is noticed that the behaviors of these corrected quark masses agrees with the previous discussion in Figs. 4 and 5.

To identify the magnetic field effect on the effective quark mass at high temperature region, in Fig. 7 we show the rescaled $T_c - eB$ phase diagram in case I, II, and III with and without the consideration of finite pionic velocities, compared with the mean field result. In the upper panel with constant pion propagating velocities, the critical temperature in different cases is as follows: case 0 (mean field): $T_c(0) = 157.2$ MeV, case I: $T_c(0) = 163.5$ MeV, case II: $T_c(0) = 159.8$ MeV, case III: $T_c(0) = 151.6$ MeV; and in the lower panel with finite pion propagating velocities case 0: $T_c(0) = 157.2$ MeV, case I: $T_c(0) = 145.3$ MeV, case II: $T_c(0) = 139.5$ MeV, case III: $T_c(0) = 135.6$ MeV. The critical temperature T_c is determined by the fastest drop of effective quark mass $\partial^2 m_q(T_c, eB)/\partial T^2 = 0$. It is noticed that in case I where we only include the feedback effect from π_0, the increasing rate of critical temperature is weakened but the system is still magnetic catalytic. However, if we include the charged pions contribution, the increasing rate of critical temperature get enhanced. Once we consider the finite velocity effect, both the enhancement from charged pions and the weakening from neutral pion to magnetic catalysis are suppressed, just as discussed in Fig. 5.

In the previous study of beyond-mean field calculation [19,62,63], IMC is achieved when a neutral pion with finite velocity is included into the system, due to the magnetic inhibition effect where the splitting between the longitudinal and transverse velocities get larger as the magnetic field and temperature are increasing. However, our calculation in this work gives an opposite result: Whether or not the influence of finite velocities is taken into account, the system remains magnetic catalytic. The main difference between the previous study and this work is that, the previous study works in the chiral limit and in this work the chiral symmetry is explicitly broken. For transverse velocity, both previous and our present result share the same form, but for longitudinal velocity, the chiral limit version is set to be the speed of light since it is a massless particle, unlike our cases, where the splitting in velocities induced by magnetic field will be thermalized once the temperature goes near the critical temperature.

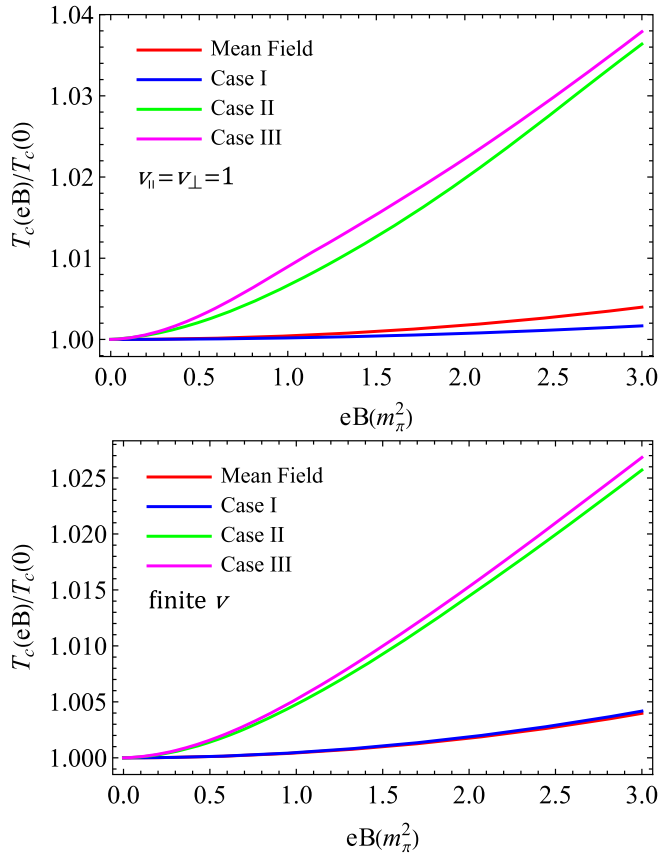

FIG. 7. Critical temperature for chiral symmetry restoration phase transition in mean field approximation and three different cases beyond mean field as a function of magnetic field, normalized by vanishing magnetic field critical temperature, considering both constant pion propagating velocities (ratios) (upper panel) and finite pion propagating velocities (ratios) (lower panel).

C. Magnetic susceptibility

Recently the lattice QCD calculation showed that the magnetized QCD matter exhibits diamagnetism at low temperature and paramagnetism at high temperature, so in this work we also calculate the magnetic susceptibility in the NJL model beyond mean field.

The magnetic susceptibility is defined by

$$\bar{\chi}(T) = -\frac{\partial^2 \Omega(T, eB)}{\partial eB^2}\bigg|_{eB=0}. \tag{38}$$

In lattice calculation, the renormalization scale choice fixes $\bar{\chi}(0) = 0$ so that the divergence in vacuum magnetic susceptibility can be eliminated. Mimicking their procedure,

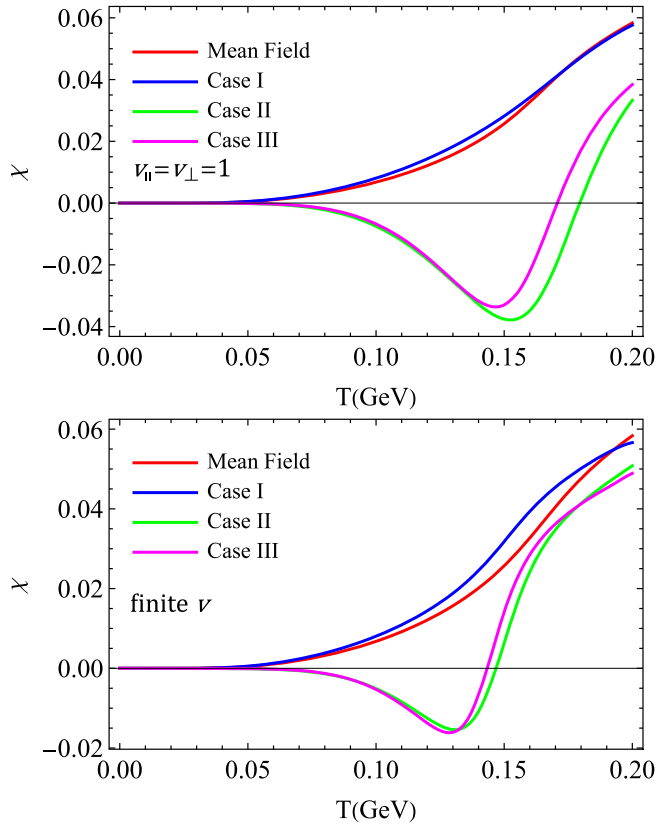

FIG. 8. Magnetic susceptibility in mean field approximation (red solid lines), beyond mean field with the feedback from π_0 (blue solid lines), $\pi_\pm$ (green solid lines), and π_0, $\pi_\pm$ (cyan solid lines) as a function of temperature with vanishing magnetic field. Propagating velocity for pions are set to be speed of light in upper panel, and finite velocities effect is considered in lower panel.

we define a new magnetic susceptibility to ensure the relation $\chi(0) = 0$, where

$$\chi(T) = \bar{\chi}(T) - \bar{\chi}(0) = \left.\frac{\partial^2 \Delta(T, eB)}{\partial eB^2}\right|_{eB=0}, \tag{39}$$

with

$$\Delta(T, eB) = \Omega(0, eB) - \Omega(T, eB). \tag{40}$$

We numerically calculate the magnetic susceptibility in the vicinity of $B = 0$, and show it in Fig. 8. In mean field approximation, the magnetic susceptibility is always positive and increases with temperature. In the case I where π_0 is included, there is no qualitative change in the behavior of magnetic susceptibility, but instead quantitatively it is enhanced by the feedback effect of π_0. However, if we include the effect of charged pions as well like in case II and case III, the magnetic susceptibility is negative at low temperature and becomes positive at high temperature region, showing qualitative agreement with the lattice result.

In the mean field approximation, the system only consists of quark, a charged particle with nonzero spin, which means its magnetic susceptibility is subject to two different mechanisms, namely Pauli paramagnetism and Landau diamagnetism [74,75]. The former originate from the spin distribution in the presence of magnetic field, and the latter is a quantum effect that is related to the cyclotron motion of charged particles. Normally the Pauli paramatnetism is stronger than Landau diamagnetism, making the total magnetic susceptibility positive in the mean field approximation. However, the pseudo-scalar particles $\pi_\pm$ are spin-0 and only subject to Landau diamagnetism, giving a negative magnetic susceptibility result. When we go beyond mean field approximation, we actually consider a system composed of quarks and mesons. At low temperature, the pion meson contribution is dominant and the total magnetic susceptibility is negative, while at high temperature, the dominance of quark contribution makes the system going back to paramagnetism.

IV. CONCLUSION

In this work, we investigated the magnetic field effect on the phase transition of chiral symmetry restoration in the framework of $SU(2)$ NJL model beyond mean field approximation. We consider three cases, by separately including the effect of π_0 (case I), $\pi_\pm$ (case II), and all three pions altogether (case III). Since sigma meson is much heavier than pions and it is not directly influenced by the magnetic field, we neglect its contribution in the calculation. To identify the effect of finite pionic propagating velocities, we consider two situations, one setting pion velocity to be exactly speed of light, and another with finite velocities determined by Eq. (30). Unlike the previous IMC results in the chiral limit due to the magnetic inhibition effect where the splitting between the longitudinal and transverse velocities of pion suppressed the critical temperature, in this work in the chiral symmetry explicitly broken case, the system is always magnetic catalytic. In the discussion of effective coupling, we notice that in absence of magnetic field, both neutral and charged pions share the same contribution to the system. However, when a magnetic field is introduced, due to the opposite response of charged and neutral pion masses to it, the feedback from π_0 weakens the MC but that from $\pi_\pm$ instead enhances it. Once we consider the effect from finite velocities, it will counter the effect from the changes in pionic pole mass. When we go to finite temperature region, all the effect above will be thermalized, resulting that IMC cannot be observed in any of the above scenarios. One problem in the calculation is in Eq. (33) where we consider a propagating velocity of $\pi_\pm$ from weak field expansion in the energy dispersion relation in strong-field formulation, since the transverse velocity here is ill-defined with momentum in corresponding direction becoming quantized Landau levels. In our future work, we plan to do the calculation in a more self-consistent way, e.g., rewrite Eq. (33) in weak-field expansion manner.

We also calculate the magnetic susceptibility in these three scenarios. In mean field approximation and only including π_0 scenario, the magnetic susceptibility is always positive and increases with temperature. However, if we include the effect of charged pions, the magnetic susceptibility becomes negative at low temperature and positive at high temperature region, showing qualitative agreement with the lattice result. A system composed of quarks is governed by both Landau diamagnetism and Pauli paramagnetism. The former originates from the spin distribution in the presence of magnetic field, and the latter is a quantum effect which relates to the cyclotron motion of charged particles. Normally the Pauli paramagnetism is stronger than Landau diamagnetism, making the total magnetic susceptibility positive in the mean field approximation. For charged pions which is spin zero, its magnetic susceptibility is only controlled by Landau diamagnetism. In beyond mean field approximation, the system is composed of quarks and mesons, and at low temperature, the meson contribution is dominant and the total magnetic susceptibility is negative, while at high temperature, the dominance of quark contribution makes the system going back to be paramagnetic.

ACKNOWLEDGMENTS

In this work, J. M., R. W., M. H., and K. X. are supported in part by the National Natural Science Foundation of China (NSFC) Grants No. 12235016, No. 12221005, No. 12147150 and the Strategic Priority Research Program of Chinese Academy of Sciences under Grant No. XDB34030000 and Fundamental Research Funds for the Central Universities, and S. M. is supported by the NSFC Grant No. 12275204 and Fundamental Research Funds for the Central Universities.

APPENDIX A: THE SUBLEADING ORDER OF POLARIZATION FUNCTIONS

In this part we will derive the specific form of polarization function in weak field expansion. We start with the equation of $\Pi^{00}(q^2)$. For the pole mass, with the static condition, the $B=0$ contribution of the polarization function can be written as

$$\Pi^{00}(q_0^2,0) = -I_1^{(0)}(m_q^2) + q_0^2 I_2^{(0)}(m_q^2,q_0^2,0), \tag{A1}$$

and $I_2^{(0)}(m_q^2,q_0^2,0)$ is given by

$$I_2^{(0)}(m_q^2,q_0^2,0) = 2\int \frac{d^3k}{(2\pi)^3}\frac{\tanh(\frac{E_q}{2T})}{E_q(4E_q^2-q_0^2)}. \tag{A2}$$

Besides, the formula of $\Pi^{00}(0,q_i^2)$ for screening mass reads

$$\begin{aligned}\Pi^{00}(0,q_i^2) = -\frac{T}{4\pi}\sum_{l=-\infty}^{\infty}\frac{1}{\sqrt{-q_i^2}}\Bigg[&\arctan\left(\frac{2m_l}{q_i}\right)\\ &-\arctan\left(\frac{2m_l-\sqrt{-q_i^2}}{q_i}\right)\\ &+\arctan\left(\frac{2q_i}{2m_l-\sqrt{-q_i^2}}\right)\Bigg],\end{aligned} \tag{A3}$$

with $m_l^2 = m_q^2+\omega_l^2$ and Matsubara frequency $\omega_l = (2l+1)\pi T$. Here we start with Π^{20}. Substituting Eq. (2) into Eq. (22), we have

$$\begin{aligned}\Pi^{20}(q^2) &= 2i\int\frac{d^4k}{(2\pi)^4}\mathrm{Tr}_{\{s\}}\left[\gamma_5\frac{k_\perp^2(m+\not{k}_\parallel)+\not{k}_\perp(m^2-k_\parallel^2)}{(k^2-m^2)^4}\gamma_5\frac{m+\not{k}-\not{q}}{(k-q)^2-m^2}\right]\\ &= 8i\int\frac{d^4k}{(2\pi)^4}\frac{k_\perp^2[m^2-k_\parallel\cdot(k-q)_\parallel]-k_\perp\cdot(k-q)_\perp(m^2-k_\parallel^2)}{(k^2-m^2)^4[(k-q)^2-m^2]}.\end{aligned} \tag{A4}$$

To calculate the pole and screening mass in different directions in a form that is as simplified as possible, we should consider these three situations separately. For pole mass, we set the external momentum $q_\perp = q_3 = 0$ and induce a replacement $\int\frac{d^4k}{(2\pi)^4}\to iT\sum_{n=-\infty}^{\infty}\int\frac{d^3k}{(2\pi)^3}$, $k_0\to i\omega_n$ in finite temperature case, to have

$$\Pi^{20}(q_0^2,q_\perp^2=q_3^2=0) = -8T\sum_{n=-\infty}^{\infty}\int\frac{d^3k}{(2\pi)^3}\frac{(i\omega_n)q_0k_\perp^2}{[(i\omega_n)^2-E_q^2]^4\{(i\omega_n-q_0)^2-E_q^2\}}. \tag{A5}$$

One can choose to either do the summation of Matsubara frequencies numerically, or use the package MatsubaraSum to do the calculation.

For screening mass, according to [71] the Matsubara summation should be done after the integration of internal momentum. Follow the similar procedure as above, we can set $q_0 = 0$ and get

$$\Pi^{20}(q_0^2=0,q_\perp^2,q_3^2)=8i\int\frac{d^4k}{(2\pi)^4}\frac{k_\perp^2[m^2+k_3\cdot(k-q)_3]-k_\perp\cdot(k-q)_\perp(m^2+k_3^2)-k_\perp q_\perp k_0^2}{(k^2-m^2)^4[(k-q)^2-m^2]}. \tag{A6}$$

Above we introduce an integration over Feynman parameters, which is given by

$$\begin{aligned}\frac{1}{(k^2-m^2)^a[(k-q)^2-m^2]^b}&=\int_0^1 dx\frac{x^{a-1}(1-x)^{b-1}}{\{x(k^2-m^2)+(1-x)[(k-q)^2-m^2]\}^{a+b}}\times\frac{\Gamma(a+b)}{\Gamma(a)\Gamma(b)}\\&=\int_0^1 dx\frac{x^{a-1}(1-x)^{b-1}}{(l^2-\Delta)^{a+b}}\times\frac{\Gamma(a+b)}{\Gamma(a)\Gamma(b)},\end{aligned} \tag{A7}$$

where

$$\begin{aligned}\Delta&=m^2-x(1-x)q^2,\\ l&=k-(1-x)q.\end{aligned} \tag{A8}$$

Substituting Eq. (A7) into Eq. (A6), setting $k=l+(1-x)q$ and discarding all the odd powers of l, we obtain

$$\begin{aligned}&\Pi^{20}(q_0^2=0,q_\perp^2,q_3^2)\\&=-32T\sum_{n=-\infty}^{\infty}\int\frac{d^3l}{(2\pi)^3}\\&\quad\times\int_0^1 dx\frac{x^3(1-x)(-l_\perp^2q_3^2+m^2q_\perp^2+l_3^2q_\perp^2-(i\omega_n)^2q_\perp^2)}{((i\omega_n)^2-l_3^2-l_\perp^2-\Delta)^5}.\end{aligned} \tag{A9}$$

Separately set $q_\perp^2=0$ and $q_3^2=0$ and performing the integration in l, we can get the Π^{20} in longitudinal and transverse directions, accordingly,

$$\begin{aligned}&\Pi^{20}(q_0^2=q_\perp^2=0,q_3^2)\\&=-\frac{T}{8\pi}\sum_{n=-\infty}^{\infty}\int_0^1 dx\frac{x^3(1-x)q_3^2}{(\Delta-(i\omega_n)^2)^{5/2}},\\&\Pi^{20}(q_0^2=q_3^2=0,q_\perp^2)\\&=\frac{T}{16\pi}\sum_{n=-\infty}^{\infty}\int_0^1 dx x^3(1-x)\\&\quad\times\left\{\frac{q_\perp^2}{(\Delta-(i\omega_n)^2)^{5/2}}+\frac{5(m^2-(i\omega_n)^2)q_\perp^2}{(\Delta-(i\omega_n)^2)^{7/2}}\right\}.\end{aligned} \tag{A10}$$

Following the similar procedure, we can get the expression for Π^{11}:

$$\begin{aligned}\Pi^{11}(q_\perp^2=q_3^2=0,q_0^2)&=4T\sum_{n=-\infty}^{\infty}\int\frac{d^3k}{(2\pi)^3}\frac{m^2+k_3^2-(i\omega_n)(i\omega_n-q_0)}{[(i\omega_n)^2-E_q^2]^2\{(i\omega_n-q_0)^2-E_q^2\}^2},\\\Pi^{11}(q_0^2=q_\perp^2=0,q_3^2)&=\frac{T}{8\pi}\sum_{n=-\infty}^{\infty}\int_0^1 dx\,x(1-x)\left\{\frac{1}{(\Delta-(i\omega_n)^2)^{3/2}}+\frac{3[m^2-x(1-x)q_3^2-(i\omega_n)^2]}{(\Delta-(i\omega_n)^2)^{5/2}}\right\},\\\Pi^{11}(q_0^2=q_3^2=0,q_\perp^2)&=\frac{T}{8\pi}\sum_{n=-\infty}^{\infty}\int_0^1 dx\,x(1-x)\left\{\frac{1}{(\Delta-(i\omega_n)^2)^{3/2}}+\frac{3[m^2-(i\omega_n)^2]}{(\Delta-(i\omega_n)^2)^{5/2}}\right\}.\end{aligned} \tag{A11}$$

For vanishing temperature case, the subleading order Π^{02} and Π^{11} have the form

$$\begin{aligned}\Pi^{20}(q_\parallel^2,q_\perp^2)(T=0)&=\frac{1}{6\pi^2}\int_0^1 dx\frac{x^3(1-x)}{\Delta^3}(2m_q^2q_\perp^2+(q_\perp^2+q_\parallel^2)\Delta),\\\Pi^{11}(q_\parallel^2,q_\perp^2)(T=0)&=\frac{1}{4\pi^2}\int_0^1 dx\frac{x(1-x)}{\Delta^2}(m_q^2+x(1-x)q_\parallel^2+\Delta),\end{aligned} \tag{A12}$$

The above expression works well in calculating both pole and screening masses for pions.

APPENDIX B: INCLUSION OF VELOCITY (RATIO)

In this section we try to understand the propagating velocity (or ratio) given in Eqs. (31) and (33) better with a demonstrative analysis on the propagator of a meson particle.

First, let us consider the 2-point correlation function (the inverse of propagator) for a meson in Euclidean space without magnetic fields

$$\Gamma^{(2)} = Z_0 p_0^2 + Z_{\vec{p}} \vec{p}^2 + m_0^2. \tag{B1}$$

Here Z_0 and $Z_{\vec{p}}$ denote the temporal and spatial wave function renormalizations, and m_0 are bare meson mass. The pole mass and screening masses are defined as [76]

$$\Gamma^{(2)}(p_0 = i m_{\rm pole}, \vec{p} = 0) = 0, \tag{B2}$$

$$\Gamma^{(2)}(p_0 = 0, \vec{p}^2 = -m_{\rm scr}^2) = 0. \tag{B3}$$

By solving the equations above, we get

$$Z_0 = \frac{m_0^2}{m_{\rm pole}^2}, \qquad Z_{\vec{p}} = \frac{m_0^2}{m_{\rm scr}^2}, \tag{B4}$$

the ratio of the temporal and spatial wave function renormalizations is

$$v \equiv \sqrt{\frac{Z_{\vec{p}}}{Z_0}} = \frac{m_{\rm pole}}{m_{\rm scr}}, \tag{B5}$$

That is Eq. (30) in our paper. The energy dispersion relation is

$$E = \sqrt{m_{\rm pole}^2 + v^2 \vec{p}^2}. \tag{B6}$$

Then, we consider the translational invariant part of the propagator for a charged scalar meson under magnetic fields in the Schwinger scheme:

$$G(p) = \int_0^\infty \frac{ids}{\cos(qBs)} \exp\left(-is\left(Z_0 p_0^2 + Z_3 p_3^2 + Z_\perp p_\perp^2 \frac{\tan(qBs)}{qBs} + m_0^2\right)\right), \tag{B7}$$

we make the change of variable $s \to -i\tau/(qB)$

$$G(p) = \frac{1}{qB}\int_0^\infty \frac{d\tau}{\cos(-i\tau)} \exp\left(-\frac{\tau}{qB}\left(Z_0 p_0^2 + Z_3 p_3^2 + Z_\perp p_\perp^2 \frac{\tan(-i\tau)}{-i\tau} + m_0^2\right)\right). \tag{B8}$$

By using

$$\cos(i\tau) = \frac{e^\tau + e^{-\tau}}{2}, \qquad i\tan(-i\tau) = \frac{e^\tau - e^{-\tau}}{e^\tau + e^{-\tau}}, \tag{B9}$$

and the generating function of the Laguerre polynomials

$$\frac{\exp(-xz/(1-z))}{1-z} = \sum_{l=0}^\infty L_l(x) z^l, \tag{B10}$$

we arrive

$$\begin{aligned} G(p) &= \frac{2}{qB}\sum_{l=0}^\infty L_l\left(\frac{Z_\perp p_\perp^2}{qB}\right)(-1)^l e^{-\frac{Z_\perp p_\perp^2}{qB}} \\ &\quad \times \int_0^\infty d\tau \exp\left(-\frac{\tau}{qB}(Z_0 p_0^2 + Z_3 p_3^2 + (2l+1)qB + m_0^2)\right) \\ &= \frac{2}{qB}\sum_{l=0}^\infty L_l\left(\frac{Z_\perp p_\perp^2}{qB}\right)(-1)^l e^{-\frac{Z_\perp p_\perp^2}{qB}} \\ &\quad \times \frac{qB}{Z_0 p_0^2 + Z_3 p_3^2 + (2l+1)qB + m_0^2}. \end{aligned} \tag{B11}$$

The energy dispersion relation reads

$$E = \sqrt{\frac{m_0^2 + Z_3 p_3^2 + (2l+1)qB}{Z_0}}, \tag{B12}$$

where $m_0/\sqrt{Z_0}$ is $m_{\pi_\pm}$ in this version of our article. Here, all the Landau levels comes with a coefficient $1/Z_0$.

It should be mentioned that above is only a demonstrative analysis. In NJL model, since pions are composite particles, the value of Z_0 cannot be determined, and we use the $v_\perp^2$ as in Eq. (33) for the coefficients before the Landau levels instead.

[1] F. Preis, A. Rebhan, and A. Schmitt, Inverse magnetic catalysis in field theory and gauge-gravity duality, Lect. Notes Phys. **871**, 51 (2013).

[2] R. Gatto and M. Ruggieri, Quark matter in a strong magnetic background, Lect. Notes Phys. **871**, 87 (2013).

[3] M. D'Elia, Lattice QCD simulations in external background fields, Lect. Notes Phys. **871**, 181 (2013).

[4] V. A. Miransky and I. A. Shovkovy, Quantum field theory in a magnetic field: From quantum chromodynamics to graphene and Dirac semimetals, Phys. Rep. **576**, 1 (2015).

[5] J. O. Andersen, W. R. Naylor, and A. Tranberg, Phase diagram of QCD in a magnetic field: A review, Rev. Mod. Phys. **88**, 025001 (2016).

[6] D. E. Kharzeev, L. D. McLerran, and H. J. Warringa, The effects of topological charge change in heavy ion collisions: "Event by event P and *CP* violation", Nucl. Phys. **A803**, 227 (2008).

[7] U. Gursoy, D. Kharzeev, and K. Rajagopal, Magnetohydrodynamics, charged currents and directed flow in heavy ion collisions, Phys. Rev. C **89**, 054905 (2014).

[8] V. de la Incera, Nonperturbative physics in a magnetic field, AIP Conf. Proc. **1361**, 74 (2011).

[9] R. C. Duncan and C. Thompson, Formation of very strongly magnetized neutron stars—implications for gamma-ray bursts, Astrophys. J. Lett. **392**, L9 (1992).

[10] H. Li, X.-L. Xia, X.-G. Huang, and H. Z. Huang, Dynamic calculations of magnetic field and implications on spin polarization and spin alignment in heavy ion collisions, Phys. Rev. C **108**, 044902 (2023).

[11] G. S. Bali *et al.*, Thermodynamic properties of QCD in external magnetic fields, Proc. Sci. ConfinementX2012 (**2012**) 197 [arXiv:1301.5826].

[12] V. G. Bornyakov, P. V. Buividovich, N. Cundy, O. A. Kochetkov, and A. Schäfer, Deconfinement transition in two-flavor lattice QCD with dynamical overlap fermions in an external magnetic field, Phys. Rev. D **90**, 034501 (2014).

[13] M. D'Elia, F. Manigrasso, F. Negro, and F. Sanfilippo, QCD phase diagram in a magnetic background for different values of the pion mass, Phys. Rev. D **98**, 054509 (2018).

[14] G. Endrodi, Critical point in the QCD phase diagram for extremely strong background magnetic fields, J. High Energy Phys. 07 (2015) 173.

[15] G. Endrodi, M. Giordano, S. D. Katz, T. G. Kovács, and F. Pittler, Magnetic catalysis and inverse catalysis for heavy pions, J. High Energy Phys. 07 (2019) 007.

[16] G. S. Bali, G. Endrődi, and S. Piemonte, Magnetic susceptibility of QCD matter and its decomposition from the lattice, J. High Energy Phys. 07 (2020) 183.

[17] S. P. Klevansky and R. H. Lemmer, Chiral symmetry restoration in the Nambu-Jona-Lasinio model with a constant electromagnetic field, Phys. Rev. D **39**, 3478 (1989).

[18] V. P. Gusynin, V. A. Miransky, and I. A. Shovkovy, Dimensional reduction and catalysis of dynamical symmetry breaking by a magnetic field, Nucl. Phys. **B462**, 249 (1996).

[19] K. Fukushima and Y. Hidaka, Magnetic catalysis versus magnetic inhibition, Phys. Rev. Lett. **110**, 031601 (2013).

[20] J. Chao, P. Chu, and M. Huang, Inverse magnetic catalysis induced by sphalerons, Phys. Rev. D **88**, 054009 (2013).

[21] L. Yu, H. Liu, and M. Huang, Spontaneous generation of local *CP* violation and inverse magnetic catalysis, Phys. Rev. D **90**, 074009 (2014).

[22] E. J. Ferrer, V. de la Incera, and X. J. Wen, Quark antiscreening at strong magnetic field and inverse magnetic catalysis, Phys. Rev. D **91**, 054006 (2015).

[23] S. Fayazbakhsh and N. Sadooghi, Anomalous magnetic moment of hot quarks, inverse magnetic catalysis, and reentrance of the chiral symmetry broken phase, Phys. Rev. D **90**, 105030 (2014).

[24] J. Mei and S. Mao, Inverse catalysis effect of the quark anomalous magnetic moment to chiral restoration and deconfinement phase transitions, Phys. Rev. D **102**, 114035 (2020).

[25] K. Xu, J. Chao, and M. Huang, Effect of the anomalous magnetic moment of quarks on magnetized QCD matter and meson spectra, Phys. Rev. D **103**, 076015 (2021).

[26] F. Lin, K. Xu, and M. Huang, Magnetism of QCD matter and the pion mass from tensor-type spin polarization and the anomalous magnetic moment of quarks, Phys. Rev. D **106**, 016005 (2022).

[27] M. Kawaguchi and M. Huang, Restriction on the form of the quark anomalous magnetic moment from lattice QCD results, Chin. Phys. C **47**, 064103 (2023).

[28] W. R. Tavares, S. S. Avancini, R. L. S. Farias, and R. P. Cardoso, Artificial first-order phase transition in a magnetized Nambu–Jona-Lasinio model with a quark anomalous magnetic moment, Phys. Rev. D **109**, 016011 (2024).

[29] N. Chaudhuri, S. Ghosh, P. Roy, and S. Sarkar, Collective modes of a massive fermion in a magnetized medium with finite anomalous magnetic moment, Phys. Rev. D **108**, 116006 (2023).

[30] C. A. Islam, M. S. Ali, and M. Huang, Deciding on the anomalous magnetic moment of quarks in a framework of nonlocal NJL model, arXiv:2302.00696.

[31] M. Ferreira, P. Costa, O. Lourenço, T. Frederico, and C. Providência, Inverse magnetic catalysis in the $(2+1)$-flavor Nambu-Jona-Lasinio and Polyakov-Nambu-Jona-Lasinio models, Phys. Rev. D **89**, 116011 (2014).

[32] H. Liu, L. Yu, M. Chernodub, and M. Huang, Possible formation of high temperature superconductor at an early stage of heavy-ion collisions, Phys. Rev. D **94**, 113006 (2016).

[33] S. S. Avancini, R. L. S. Farias, M. Benghi Pinto, W. R. Tavares, and V. S. Timóteo, π_0 pole mass calculation in a strong magnetic field and lattice constraints, Phys. Lett. B **767**, 247 (2017).

[34] A. Ayala, C. A. Dominguez, L. A. Hernandez, M. Loewe, A. Raya, J. C. Rojas, and C. Villavicencio, Thermomagnetic properties of the strong coupling in the local Nambu–Jona-Lasinio model, Phys. Rev. D **94**, 054019 (2016).

[35] R. L. S. Farias, V. S. Timoteo, S. S. Avancini, M. B. Pinto, and G. Krein, Thermo-magnetic effects in quark matter: Nambu–Jona-Lasinio model constrained by lattice QCD, Eur. Phys. J. A **53**, 101 (2017).

[36] X. Chen, L. Zhang, and D. Hou, Running coupling constant at finite chemical potential and magnetic field from holography, Chin. Phys. C **46**, 073101 (2022).

[37] B.-k. Sheng, X. Wang, and L. Yu, Impacts of inverse magnetic catalysis on screening masses of neutral pions

and sigma mesons in hot and magnetized quark matter, Phys. Rev. D **105**, 034003 (2022).
[38] S. Mao and Y. Tian, Pion superfluid phase transition under an external magnetic field including the inverse magnetic catalysis effect, Phys. Rev. D **106**, 094017 (2022).
[39] K. Kamikado and T. Kanazawa, Magnetic susceptibility of a strongly interacting thermal medium with $2+1$ quark flavors, J. High Energy Phys. 01 (2015) 129.
[40] B. Sahoo, K. K. Pradhan, D. Sahu, and R. Sahoo, Effect of a magnetic field on the thermodynamic properties of a high-temperature hadron resonance gas with van der Waals interactions, Phys. Rev. D **108**, 074028 (2023).
[41] R. Wen, S. Yin, W.-j. Fu, and M. Huang, Functional renormalization group study of neutral and charged pions in magnetic fields in the quark-meson model, Phys. Rev. D **108**, 076020 (2023).
[42] X. Li, W.-j. Fu, and Y.-x. Liu, Thermodynamics of $2+1$ flavor Polyakov-loop quark-meson model under external magnetic field, Phys. Rev. D **99**, 074029 (2019).
[43] K. Kamikado and T. Kanazawa, Chiral dynamics in a magnetic field from the functional renormalization group, J. High Energy Phys. 03 (2014) 009.
[44] K. Fukushima and J. M. Pawlowski, Magnetic catalysis in hot and dense quark matter and quantum fluctuations, Phys. Rev. D **86**, 076013 (2012).
[45] W.-j. Fu and Y.-x. Liu, Four-fermion interactions and the chiral symmetry breaking in an external magnetic field, Phys. Rev. D **96**, 074019 (2017).
[46] H. Bohra, D. Dudal, A. Hajilou, and S. Mahapatra, Anisotropic string tensions and inversely magnetic catalyzed deconfinement from a dynamical AdS/QCD model, Phys. Lett. B **801**, 135184 (2020).
[47] H. Bohra, D. Dudal, A. Hajilou, and S. Mahapatra, Chiral transition in the probe approximation from an Einstein-Maxwell-dilaton gravity model, Phys. Rev. D **103**, 086021 (2021).
[48] N. Wen, X. Cao, J. Chao, and H. Liu, Neutral pion masses within a hot and magnetized medium in a lattice-improved soft-wall AdS/QCD model, Phys. Rev. D **109**, 086021 (2024).
[49] N. Mueller, J. A. Bonnet, and C. S. Fischer, Dynamical quark mass generation in a strong external magnetic field, Phys. Rev. D **89**, 094023 (2014).
[50] N. Mueller and J. M. Pawlowski, Magnetic catalysis and inverse magnetic catalysis in QCD, Phys. Rev. D **91**, 116010 (2015).
[51] J. Braun, W. A. Mian, and S. Rechenberger, Delayed magnetic catalysis, Phys. Lett. B **755**, 265 (2016).
[52] S. P. Klevansky, The Nambu-Jona-Lasinio model of quantum chromodynamics, Rev. Mod. Phys. **64**, 649 (1992).
[53] E. Quack and S. P. Klevansky, Effective $1/N_c$ expansion in the NJL model, Phys. Rev. C **49**, 3283 (1994).
[54] P. Zhuang, J. Hufner, and S. P. Klevansky, Thermodynamics of a quark—meson plasma in the Nambu-Jona-Lasinio model, Nucl. Phys. **A576**, 525 (1994).
[55] S. Mao, Pions in magnetic field at finite temperature, Phys. Rev. D **99**, 056005 (2019).
[56] L. Li and S. Mao, Light mesons around critical end points in $T-\mu_B-\mu_I-eB$ space, Chin. Phys. C **46**, 094105 (2022).
[57] J. Mei, T. Xia, and S. Mao, Mass spectra of neutral mesons $K0, \pi 0, \eta, \eta'$ at finite magnetic field, temperature and quark chemical potential, Phys. Rev. D **107**, 074018 (2023).
[58] H. Liu, X. Wang, L. Yu, and M. Huang, Neutral and charged scalar mesons, pseudoscalar mesons, and diquarks in magnetic fields, Phys. Rev. D **97**, 076008 (2018).
[59] M. Coppola, D. Gomez Dumm, S. Noguera, and N. N. Scoccola, Neutral and charged pion properties under strong magnetic fields in the NJL model, Phys. Rev. D **100**, 054014 (2019).
[60] S. S. Avancini, M. Coppola, N. N. Scoccola, and J. C. Sodré, Light pseudoscalar meson masses under strong magnetic fields within the SU(3) Nambu–Jona-Lasinio model, Phys. Rev. D **104**, 094040 (2021).
[61] L. Li and S. Mao, Inverse magnetic catalysis effect and current quark mass effect on mass spectra and Mott transitions of pions under external magnetic field, Phys. Rev. D **108**, 054001 (2023).
[62] S. Mao, Inverse magnetic catalysis in Nambu–Jona-Lasinio model beyond mean field, Phys. Lett. B **758**, 195 (2016).
[63] S. Mao, Chiral symmetry restoration and quark deconfinement beyond mean field in a magnetized PNJL model, Phys. Rev. D **97**, 011501 (2018).
[64] D. Gomez Dumm, S. Noguera, and N. N. Scoccola, Charged meson masses under strong magnetic fields: Gauge invariance and Schwinger phases, Phys. Rev. D **108**, 016012 (2023).
[65] W.-j. Fu, C. Huang, J. M. Pawlowski, and Y.-y. Tan, Four-quark scatterings in QCD I, SciPost Phys. **14**, 069 (2023).
[66] W.-j. Fu, C. Huang, J. M. Pawlowski, and Y.-y. Tan, Four-quark scatterings in QCD II, arXiv:2401.07638.
[67] E. V. Shuryak, Physics of the pion liquid, Phys. Rev. D **42**, 1764 (1990).
[68] R. D. Pisarski and M. Tytgat, Propagation of cool pions, Phys. Rev. D **54**, R2989 (1996).
[69] S. Fayazbakhsh, S. Sadeghian, and N. Sadooghi, Properties of neutral mesons in a hot and magnetized quark matter, Phys. Rev. D **86**, 085042 (2012).
[70] S. Fayazbakhsh and N. Sadooghi, Weak decay constant of neutral pions in a hot and magnetized quark matter, Phys. Rev. D **88**, 065030 (2013).
[71] B. Sheng, Y. Wang, X. Wang, and L. Yu, Pole and screening masses of neutral pions in a hot and magnetized medium: A comprehensive study in the Nambu–Jona-Lasinio model, Phys. Rev. D **103**, 094001 (2021).
[72] M. Huang, P.-f. Zhuang, and W.-q. Chao, Massive meson fluctuation in NJL model, Commun. Theor. Phys. **34**, 91 (2000).
[73] M. Oertel, M. Buballa, and J. Wambach, Meson loop effects in the NJL model at zero and nonzero temperature, Phys. At. Nucl. **64**, 698 (2001).
[74] L. Landau, Diamagnetismus der Metalle, Z. Phys. **64**, 629 (1930).
[75] L. Landau and E. Lifshitz, in *Statistical Physics*, 3rd ed. (Butterworth-Heinemann, Oxford, 1980), pp. 158–190.
[76] A. J. Helmboldt, J. M. Pawlowski, and N. Strodthoff, Towards quantitative precision in the chiral crossover: Masses and fluctuation scales, Phys. Rev. D **91**, 054010 (2015).